

Nonlinear Control of an Electrohydraulic Velocity Servosystem

Mihailo Jovanović
jmihailo@engineering.ucsb.edu

Department of Mechanical and Environmental Engineering
University of California, Santa Barbara, CA 93106-5070

Abstract

This paper addresses the analysis and control of an electrohydraulic velocity servosystem in the presence of flow nonlinearities and internal friction. Two different nonlinear design procedures are employed: feedback linearization and backstepping. It is shown that both these techniques can be successfully used to stabilize any chosen operating point of the system. Additionally, invaluable new insights are gained about the dynamics of the system under consideration. This illustrates that the true potential of constructive nonlinear design lies far beyond the mere task of achieving a desired control objective. All derived results are validated by computer simulation of a nonlinear mathematical model of the system.

1 Introduction

Electrohydraulic servosystems (EHSS) are encountered in a wide range of modern industrial applications because of their ability to handle large inertia and torque loads and, at the same time, achieve fast responses and a high degree of both accuracy and performance [1, 2]. Typical applications include active suspension systems, control of industrial robots, and processing of plastic. They are also ubiquitous in commercial aircrafts, satellites, launch vehicles, flight simulators, turbine control, and numerous military applications. The electronic components provide the desired flexibility, while the hydraulic part of an EHSS is responsible for successful power management. The main components of the power assembly of an EHSS are its hydraulic power supply, electrohydraulic servovalve, and hydraulic actuator. In practice, these devices are usually actuated by hydraulic cylinders and hydraulic motors.

Depending on the desired control objective, an EHSS can be classified as either a position, velocity or force/torque EHSS. Among these the position control has received by far the most attention in the literature. However, most of the solutions have been based on classical linear control theory or feedback linearization technique, despite the fact that the underlying dynamics are nonlinear with inevitable modeling uncertainties. Two recent articles by Yao *et.al.* [3] and Alleyne and Liu [4] addressed these important issues¹. In [3], Yao *et.al.* used a discontinuous projection-based adaptive robust controller that takes into account the effect of both parametric uncertainties and some nonlinearities. In [4], Alleyne and Liu developed a control strategy that guarantees global stability of nonlinear,

¹The interested reader is referred to the references contained therein for a more complete picture.

minimum phase single-input single-output (SISO) systems in the strict feedback form by using a passivity approach and they later used this strategy to control the pressure of an EHSS. Both these articles illustrate that control of an EHSS is still a very research-intensive area and that significant improvement in the dynamical behavior of EHSS can be accomplished using nonlinear control algorithms.

This paper investigates the control of a velocity EHSS whose mathematical model accounts for flow nonlinearities and internal friction. The main components of the system that we study are axial-piston hydraulic motor and electrohydraulic servovalve. It is shown that this system has a well defined *relative degree* and no non-trivial *zero dynamics*. The latter property illustrates that our system is, by definition, *minimum phase* which allows application of many different design tools. In particular, a stabilizing controller has been designed using the technique of feedback linearization. Despite the fact that this controller successfully achieves the desired objectives, another controller is designed using the backstepping approach, which avoids unnecessary cancellations that can have a detrimental effect in the presence of parametric uncertainties and/or unmodeled dynamics. It is further illustrated, using the backstepping procedure, that not only has the desired control objective been accomplished, but also, that a new physical intuition about the dynamics of EHSS has been developed. This is to some degree a surprising discovery which additionally shows the power of constructive nonlinear design procedures. The performance of all designed controllers is validated by the appropriate simulation of a nonlinear mathematical model of the system.

Feedback linearization and backstepping are well-studied design tools [5, 6, 7] but they have not been applied to control of a velocity EHSS to the best of the author's knowledge. Feedback linearization employs a change of coordinates and feedback control to transform a given nonlinear system into an equivalent linear system [5]. A major caveat of feedback linearization approach is related to the cancellations that are introduced in the design process. Namely, this design philosophy does not make use of 'beneficial nonlinearities' and can lead to instability in the presence of modeling uncertainties. On the other hand, backstepping represents a recursive design scheme that can be used for systems in strict-feedback form with nonlinearities not constrained by linear bounds [6, 7]. At every step of backstepping a new Control Lyapunov Function (CLF) is constructed by augmentation of the CLF from the

previous step by a term which penalizes the error between 'virtual control' and its desired value (so-called 'stabilizing function'). A major advantage of backstepping is the construction of a Lyapunov function whose derivative can be made negative definite by a variety of control laws rather than by a specific control law [7]. Additionally, as a design tool, backstepping is less restrictive than feedback linearization and its previously mentioned designed flexibility can put 'beneficial nonlinearities' to good use.

The paper is organized as follows: In section 2, EHSS and its nonlinear mathematical model are described. In section 3, structural properties of the system, such as nonlinear *relative degree* and *zero dynamics*, are studied and a controller is designed based on feedback linearization. In section 4, issues related to the backstepping design are discussed in some detail. In conclusion, section 5 summarizes major contributions and future research directions.

2 System Description

A schematic of an electrohydraulic velocity servosystem is shown in Figure 1.

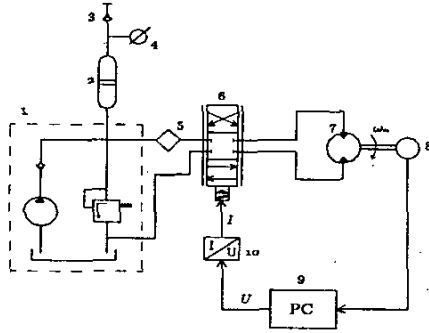


Figure 1: Electrohydraulic velocity servosystem.

The basic parts of this system are: 1. hydraulic power supply, 2. accumulator, 3. charge valve, 4. pressure gauge device, 5. filter, 6. two-stage electrohydraulic servovalve, 7. hydraulic motor, 8. measurement device, 9. personal computer, and 10. voltage-to-current converter.

The states of the system shown in Figure 1 are measured and they are forwarded to the personal computer. Electric voltage signal is generated based on this information according to the designed control law and it is converted to the current by voltage-to-current converter. This signal acts on the electrohydraulic servovalve which in turn supplies the hydraulic motor with appropriate amount of oil.

A mathematical representation of the system is derived in [8] using Newton's Second Law for the rotational motion of the motor shaft, the continuity equation for each chamber of the hydraulic motor, and by approximating the connection between the torque motor and the first stage of the electrohydraulic servovalve by a first order transfer function. This representation accounts for flow nonlinearities and internal friction. If the state

variables are denoted by: x_1 - hydro motor angular velocity, [rad/s], x_2 - load pressure differential, [Pa], and x_3 - valve displacement, [m], then the model of EHSS in *physical coordinates* is given by

$$\begin{aligned} \dot{x}_1 &= \frac{1}{J_t} \{-B_m x_1 + q_m x_2 - q_m C_f P_S \text{sgn } x_1\}, \\ \dot{x}_2 &= \frac{2\beta_e}{V_0} \{-q_m x_1 - C_{im} x_2 + C_d W x_3 \sqrt{\frac{1}{\rho} (P_S - x_2 \text{sgn } x_3)}\}, \\ \dot{x}_3 &= \frac{1}{T_r} \{-x_3 + \frac{K_r}{K_q} u\}, \\ y &= x_1, \end{aligned} \quad (1)$$

where the *nominal* values of the parameters appearing in equation (1) are: $J_t = 0.03 \text{ kgm}^2$ - total inertia of the motor and load referred to the motor shaft, $q_m = 7.96 \times 10^{-7} \frac{\text{m}^3}{\text{rad}}$ - volumetric displacement of the motor, $B_m = 1.1 \times 10^{-3} \text{ Nms}$ - viscous damping coefficient, $C_f = 0.104$ - dimensionless internal friction coefficient, $V_0 = 1.2 \times 10^{-4} \text{ m}^3$ - average contained volume of each motor chamber, $\beta_e = 1.391 \times 10^9 \text{ Pa}$ - effective bulk modulus of the system, $C_d = 0.61$ - discharge coefficient, $C_{im} = 1.69 \times 10^{-11} \frac{\text{m}^3}{\text{Pa}\cdot\text{s}}$ - internal or cross-port leakage coefficient of the motor, $P_S = 10^7 \text{ Pa}$ - supply pressure, $\rho = 850 \frac{\text{kg}}{\text{m}^3}$ - oil density, $T_r = 0.01 \text{ s}$ - valve time constant, $K_r = 1.4 \times 10^{-4} \frac{\text{m}^3}{\text{sV}}$ - valve gain, $K_q = 1.66 \frac{\text{m}^2}{\text{s}}$ - valve flow gain, and $W = 8\pi \times 10^{-3} \text{ m}$ - surface gradient.

The control objective is stabilization of any chosen operating point of the system. It is readily shown that equilibrium points of system (1) are given by

$$\begin{aligned} x_{1N} &= \text{arbitrary constant value of our choice,} \\ x_{2N} &= \frac{1}{q_m} \{B_m x_{1N} + q_m P_S C_f\}, \\ x_{3N} &= \frac{q_m x_{1N} + C_{im} x_{2N}}{C_d W \sqrt{\frac{1}{\rho} (P_S - x_{2N})}}, \end{aligned} \quad (2)$$

while the value of the control signal necessary to keep x_3 at the equilibrium is $u_N = \frac{K_r}{K_q} x_{3N}$.

It is assumed that the motor shaft does not change its direction of rotation, $x_1 > 0$. This is a practical assumption and in order for it to be satisfied, the servovalve displacement x_3 does not have to move in both directions relative to the neutral position $x_3 = 0$. This fact allows us to restrict the entire problem to the region where $x_3 > 0$. In this case, the mathematical representation of the system simplifies to

$$\begin{aligned} \dot{x}_1 &= \frac{1}{J_t} \{-B_m x_1 + q_m x_2 - q_m C_f P_S\}, \\ \dot{x}_2 &= \frac{2\beta_e}{V_0} \{-q_m x_1 - C_{im} x_2 + C_d W x_3 \sqrt{\frac{1}{\rho} (P_S - x_2)}\}, \\ \dot{x}_3 &= \frac{1}{T_r} \{-x_3 + \frac{K_r}{K_q} u\}, \\ y &= x_1. \end{aligned} \quad (3)$$

3 Feedback linearization

In this section, structural properties of the system, such as nonlinear *relative degree* and *zero dynamics*, are in-

vestigated and a controller is designed based on feedback linearization approach. These structural properties represent a generalization of their well-known linear counterparts. Namely, the relative degree of a SISO linear system is determined as a difference between the number of poles and zeros of the corresponding transfer function. Equivalently, it is equal to the number of times that output has to be differentiated in order for the input variable to appear. On the other hand, the zero dynamics describe the internal behavior of the system when the output is identically equal to zero. The systems with asymptotically stable zero dynamics are referred to as the *minimum phase systems* and they are much easier to control than the systems whose zero dynamics is not stable. It is shown that our system has good structural properties: well defined relative degree and no nontrivial zero dynamics. These features imply that EHSS lends itself to numerous available design tools.

3.1 Relative Degree and Zero Dynamics

The mathematical model of the system can be rewritten as

$$\begin{aligned}\dot{x} &= \bar{f}(x) + \bar{g}(x)u, \\ y &= \bar{h}(x),\end{aligned}\quad (4)$$

by defining $x := [x_1 \ x_2 \ x_3]'$, $\bar{f} := [\bar{f}_1 \ \bar{f}_2 \ \bar{f}_3]'$, $\bar{g} := [0 \ 0 \ K_r/(K_q T_r)]'$, $\bar{h} := x_1$, and

$$\begin{aligned}\bar{f}_1 &:= \frac{1}{J_t} \{-B_m x_1 + q_m x_2 - q_m C_f P_S\}, \\ \bar{f}_2 &:= \frac{2\beta_e}{V_0} \{-q_m x_1 - C_{im} x_2 + C_d W x_3 \sqrt{\frac{1}{\rho}(P_S - x_2)}\}, \\ \bar{f}_3 &:= -\frac{1}{T_r} x_3.\end{aligned}$$

In order to determine *relative degree*, the output should be differentiated a sufficient number of times [5]. The first derivative of $y = \bar{h}(x)$ is given by

$$\begin{aligned}\dot{y} &= \frac{1}{J_t} \{-B_m x_1 + q_m x_2 - q_m C_f P_S\} + 0 \cdot u \\ &=: L_{\bar{f}} \bar{h}(x) + L_{\bar{g}} \bar{h}(x)u.\end{aligned}\quad (5)$$

Since the control input does not appear in (5), the output function should be differentiated one more time to yield

$$\begin{aligned}\ddot{y} &= \frac{1}{J_t} \{-B_m \bar{f}_1 + q_m \bar{f}_2\} + 0 \cdot u \\ &=: L_{\bar{f}}^2 \bar{h}(x) + L_{\bar{g}} L_{\bar{f}} \bar{h}(x)u.\end{aligned}\quad (6)$$

The absence of u in \ddot{y} requires determination of the third derivative of y as follows

$$\ddot{\ddot{y}} = L_{\bar{f}}^3 \bar{h}(x) + L_{\bar{g}} L_{\bar{f}}^2 \bar{h}(x)u, \quad (7)$$

where

$$\begin{aligned}L_{\bar{f}}^3 \bar{h}(x) &= -\frac{1}{J_t} \left\{ \frac{B_m}{J_t} (-B_m \bar{f}_1 + q_m \bar{f}_2) + \frac{2\beta_e q_m}{V_0} (q_m \bar{f}_1 \right. \\ &\quad \left. + C_{im} \bar{f}_2 + \frac{C_d W x_3 (T_r \bar{f}_2 + 2(P_S - x_2))}{2T_r \sqrt{\rho(P_S - x_2)}}) \right\}\end{aligned}$$

and

$$L_{\bar{g}} L_{\bar{f}}^2 \bar{h}(x) = \frac{2q_m \beta_e C_d W K_r}{J_t V_0 K_q T_r} \sqrt{\frac{1}{\rho}(P_S - x_2)}.$$

Thus, one can conclude that $L_{\bar{g}} L_{\bar{f}}^2 \bar{h}(x) \neq 0, \forall x_2 < P_S$. Since x_2 represents the load pressure differential it can never become greater than the supply pressure. This implies that system (3) has a relative degree equal to three, $r = 3$, which is well-defined in the entire state space of physical interest.

3.2 Feedback Linearization Design

The features of EHSS discussed in §3.1 allow us to feedback linearize this system with a control law of the form

$$u = \frac{1}{L_{\bar{g}} L_{\bar{f}}^2 \bar{h}(x)} \{-L_{\bar{f}}^3 \bar{h}(x) + v\}, \quad (8)$$

where

$$\begin{aligned}v &= -k_0(x_1 - y_d) - k_1(\dot{y}_d - \dot{x}_1) \\ &\quad - k_2\left\{\frac{1}{J_t}(-B_m \bar{f}_1 + q_m \bar{f}_2) - \ddot{y}_d\right\} + \ddot{\ddot{y}}_d.\end{aligned}\quad (9)$$

Note that y_d is the desired output value which can be either time varying or constant, while k_0 , k_1 and k_2 are positive design parameters which have to satisfy $k_1 k_2 > k_0$ to guarantee stability.

Simulation results of system (3) achieved using control law (8,9) for $y_d = x_{1N} = 200 \text{ rad/s}$, $x(0) = 0$, $k_0 = 5000$, $k_1 = 5150$, and $k_2 = 151$ are shown in Figure 2. Clearly, a desired control objective is met with a reasonable control effort.

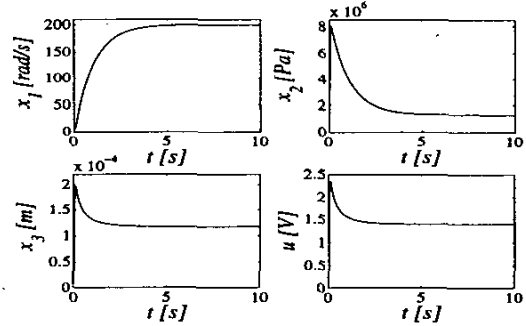


Figure 2: Simulation results of system (3) obtained using control law (8,9), for $k_0 = 5000$, $k_1 = 5150$ and $k_2 = 151$, $x_{1N} = 200 \text{ rad/s}$, and $x(0) = 0$.

Even though the proposed controller works well, its design relies heavily on cancellation of nonlinearities, which can be detrimental in the presence of parametric uncertainties and/or unmodeled dynamics. In the next section, we present a controller designed using a backstepping approach which allows us to avoid unnecessary cancellations.

4 Backstepping Design

This section addresses the problem of designing a controller which provides asymptotic stability of the operating point of interest. Assuming that the full state

information is available, the underlying technique for solving this problem is backstepping [6, 7]. Backstepping represents a powerful design tool that can be applied to the ‘lower triangular’ systems with nonlinearities not constrained by linear bounds. It is remarkable that in the process of controller design very important information about the dynamics of EHSS are obtained.

Clearly, system (3) is ‘lower triangular’ and, therefore, suitable for application of backstepping. However, before starting the design, a coordinate transformation

$$z_i := x_i - x_{iN}, \forall i = 1, 2, 3; \quad v := u - u_N, \quad (10)$$

is introduced to rewrite equation (3) in a form that would decrease the number of necessary recursive steps from three to two. In this manner, using the relationships given by (2), the model of our system in terms of these *deviation* variables takes the form

$$\begin{aligned} \dot{z}_1 &= \frac{1}{J_t} \{-B_m z_1 + q_m z_2\}, \\ \dot{z}_2 &= \frac{2\beta_e}{V_0} \{-q_m z_1 - (C_{im} + \gamma(z_2))z_2 \\ &\quad + C_d W z_3 \sqrt{\frac{1}{\rho}(P_S - x_{2N} - z_2)}\}, \\ \dot{z}_3 &= \frac{1}{T_r} \{-z_3 + \frac{K_r}{K_q} v\}, \end{aligned} \quad (11)$$

where

$$\gamma(z_2) := \frac{C_d W x_{3N}}{\sqrt{\rho(P_S - x_{2N} - z_2)} + \sqrt{\rho(P_S - x_{2N})}} > 0.$$

Careful consideration of the model (11) reveals a block-strict-feedback form. Namely, by defining vector η and scalar ξ as $\eta := [z_1 \ z_2]'$ and $\xi := z_3$, one can rewrite (11) as

$$\dot{\eta} = f(\eta) + g(\eta)\xi, \quad (12a)$$

$$\dot{\xi} = v_a, \quad (12b)$$

where $f(\eta) := [f_1 \ f_2]'$, $f_1 := \frac{1}{J_t} \{-B_m z_1 + q_m z_2\}$, $f_2 := \frac{2\beta_e}{V_0} \{-q_m z_1 - (C_{im} + \gamma(z_2))z_2\}$, $g(\eta) := [0 \ g_2]'$, $g_2 := \frac{2\beta_e}{V_0} C_d W \sqrt{\frac{1}{\rho}(P_S - x_{2N} - z_2)}$, and

$$v_a := \frac{1}{T_r} \{-z_3 + \frac{K_r}{K_q} v\}. \quad (13)$$

The system, in this form, is now amenable to be analyzed by the backstepping design methodology. In the first step, equation (12a) is stabilized by considering variable ξ as its control. Since ξ is not actually a control but, rather, a state variable, the error between ξ and the value which stabilizes (12a) must be penalized in the augmented Lyapunov function at the next step. In this way, a stabilizing control law is designed for the overall system.

Step 1 The recursive design starts with subsystem (12a) by proposing a CLF of the form

$$V_1(\eta) = \frac{1}{2} J_t z_1^2 + \frac{1}{2} \frac{V_0}{2\beta_e} z_2^2. \quad (14)$$

The derivative of $V_1(\eta)$ along the solutions of (12a) is given by

$$\dot{V}_1 = L_f V_1(\eta) + L_g V_1(\eta)\xi, \quad (15)$$

where

$$L_f V_1(\eta) = -B_m z_1^2 - (C_{im} + \gamma(z_2))z_2^2, \quad (16)$$

and

$$L_g V_1(\eta) = C_d W z_2 \sqrt{\frac{1}{\rho}(P_S - x_{2N} - z_2)}. \quad (17)$$

Based on (15) it can be concluded that $L_f V_1(\eta)$ is a negative definite function, that is,

$$W_1(\eta) := -L_f V_1(\eta) > 0, \quad \forall \eta \in \mathcal{D}, \quad (18)$$

where $\mathcal{D} \in \mathcal{R}^2$ is the region of the state space which contains all z_1 and z_2 of physical interest².

We stress that, due to the design flexibility of backstepping, we can choose a variety of ‘stabilizing functions’ $\xi_d := \alpha(\eta)$ to make \dot{V}_1 negative definite. For example, the nice properties of $L_f V_1(\eta)$ allow a choice of ‘virtual control’ identically equal to zero, $\xi_{d1} := \alpha_1(\eta) \equiv 0$. This means that, unforced nonlinear subsystem (12a) has an asymptotically stable equilibrium at $\eta = 0$. Hence, in the remainder of the design procedure, the only thing that should be taken care of is stabilization of the position of the electrohydraulic servovalve.

On the other hand, we could have chosen ‘stabilizing function’ of the form $\xi_{d2} := \alpha_2(\eta) = -k_0 z_2$, $k_0 > 0$. This particular choice of ‘virtual control’ yields

$$\begin{aligned} W_2(\eta) &:= -L_f V_1(\eta) - L_g V_1(\eta)\alpha_2(\eta) \\ &= W_1(\eta) + k_0 C_d W z_2^2 \sqrt{\frac{1}{\rho}(P_S - x_{2N} - z_2)}, \end{aligned}$$

which is clearly positive definite $\forall \eta \in \mathcal{D}$.

The above choices of ‘stabilizing functions’ are not, by any means, the only ones that would lead to negative definiteness of \dot{V}_1 along the solutions of (12a). However, they are very suitable since they avoid cancellation of nonlinearities in the first step of backstepping.

Since ξ is not actually a control but, rather, a state variable, we introduce the change of variables

$$\zeta_i := \xi - \alpha_i(\eta), \quad i = 1, 2, \quad (19)$$

which adds an additional term on the right-hand side of (15)

$$\dot{V}_1 = -W_1(\eta) + \zeta_i L_g V_1(\eta). \quad (20)$$

The second term $\zeta_i L_g V_1(\eta)$ in \dot{V}_1 would be taken care of in the second step of backstepping.

²Note that we are not interested in a global result since state variables of the system under consideration are not allowed to take all values in the state space due to physical limitations. Since we consider the case $x_1 > 0$ (i.e. $x_3 > 0$), the values that the state space variables can assume are given by $\{x_1, x_2, x_3\} \in [0, x_{1max}] \times [0, P_S] \times [0, x_{3max}]$, where $x_{1max} = 404 \text{ rad/s}$, $P_S = 10^7 \text{ Pa}$, $x_{3max} = 4 \times 10^{-4} \text{ m}$. From this, it is straightforward to see that the domain \mathcal{D} can be defined as $\mathcal{D} := [-x_{1N}, x_{1max} - x_{1N}] \times [-x_{2N}, P_S - x_{2N}]$.

Step 2 Coordinate transformation (19) renders (12b) into a form suitable for the remainder of our design

$$\dot{\zeta}_i = \dot{\xi} - \dot{\alpha}_i = v_a - \frac{\partial \alpha_i(\eta)}{\partial \eta} \dot{\eta}. \quad (21)$$

Augmentation of the CLF from Step 1 by a term which penalizes the error between ξ and $\alpha_i(\eta)$ yields a function

$$V_2(\eta, \zeta_i) := V_1(\eta) + \frac{1}{2} \zeta_i^2, \quad (22)$$

whose derivative along the solutions of

$$\begin{aligned} \dot{\eta} &= f(\eta) + g(\eta) \{\zeta_i + \alpha_i(\eta)\}, \\ \dot{\zeta}_i &= v_a - \frac{\partial \alpha_i(\eta)}{\partial \eta} \{f(\eta) + g(\eta)\xi\}, \end{aligned} \quad (23)$$

is determined by

$$\begin{aligned} \dot{V}_2 &= \dot{V}_1 + \zeta_i \dot{\zeta}_i \\ &= -W_i(\eta) + \zeta_i \{v_a + L_g V_1(\eta) - \frac{\partial \alpha_i}{\partial \eta} \{f(\eta) + g(\eta)\xi\}\}. \end{aligned}$$

With a control law of the form

$$v_{ai} = -k_1 \zeta_i - L_g V_1(\eta) + \frac{\partial \alpha_i(\eta)}{\partial \eta} \{f(\eta) + g(\eta)\xi\}, \quad (24)$$

where k_1 is a positive design parameter, \dot{V}_2 becomes a negative definite function, i.e. $\dot{V}_2 = -W_i(\eta) - k_1 \zeta_i^2 < 0$.

By combining (10), (13), (17), and (24) the control laws that correspond to stabilizing functions α_1 and α_2 , in original coordinates, are obtained as

$$\begin{aligned} u_1 &= u_N - \frac{K_q T_r}{K_r} \left\{ \left(k_1 - \frac{1}{T_r} \right) (x_3 - x_{3N}) \right. \\ &\quad \left. + C_d W(x_2 - x_{2N}) \sqrt{\frac{1}{\rho} (P_S - x_2)} \right\}, \end{aligned} \quad (25)$$

and

$$u_2 = u_1 - \frac{K_q T_r k_0}{K_r} \{k_1(x_2 - x_{2N}) + \bar{f}_2\}, \quad (26)$$

respectively, where \bar{f}_2 is defined in §3.1.

Simulation results of system (3) obtained using control laws (25) and (26), for $x(0) = 0$, $x_{1N} = 200 \text{ rad/s}$, $k_1 = 1 \text{ s}^{-1}$, and $k_0 = 10^{-7} \text{ m/Pa}$, are shown in Figure 3 and Figure 4, respectively. It can be seen that, the obtained results are very similar to each other, except for a presence of high frequency harmonics in the evolution of u_2 . The former observation can be attributed to the fact that a very small value has been assigned to a design parameter k_0 in order to avoid saturation of control³. Since u_1 represents a special case of u_2 obtained by setting k_0 to zero, the closeness of state space variables in Figure 3 and Figure 4 is reasonable.

Furthermore, both control laws attain asymptotic stability of the equilibrium points determined by (2) and do not saturate. However, one notices that, in both cases, the second state variable comes very close to the desired equilibrium level almost immediately, while

³We assume that the magnitude of the control signal at our disposal has to be between 0 and 5 V.

the output $y = x_1$ experiences lengthy transients before achieving an eventual steady state⁴. This sluggishness of the output variable seems to be caused by the long transient response of the servovalve displacement and/or the absence of terms that would penalize the output error in the control laws.

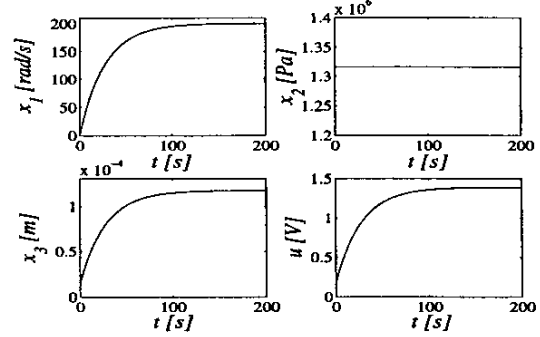


Figure 3: Simulation results of system (3) obtained using control law (25), for $k_1 = 1 \text{ s}^{-1}$, $x_{1N} = 200 \text{ rad/s}$, and $x(0) = 0$.

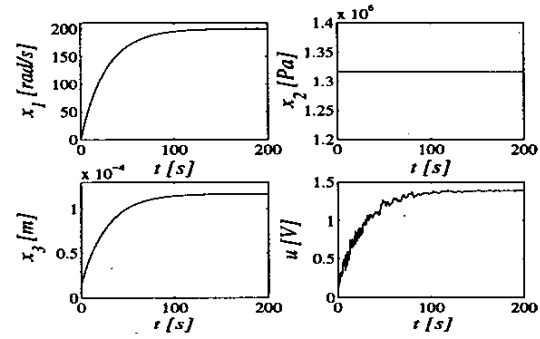


Figure 4: Simulation results of system (3) obtained using control law (26), for $k_0 = 10^{-7} \text{ m/Pa}$, $k_1 = 1 \text{ s}^{-1}$, $x_{1N} = 200 \text{ rad/s}$, and $x(0) = 0$.

This problem is circumvented by a different choice of control, where, we propose a controller corresponding to stabilizing function α_1 of the form

$$v_a = -k_2 \xi, \quad (27)$$

or equivalently, in absolute coordinates,

$$u_3 = u_N - \frac{K_q T_r}{K_r} \left(k_2 - \frac{1}{T_r} \right) (x_3 - x_{3N}), \quad (28)$$

where $k_2 > 0$ is a design parameter. One notices that the only difference between control law (25) and its counterpart (28) is the fact that the latter does not contain the term $-L_g V_1(\eta)$. This means that the derivative of the proposed Lyapunov function along the solutions of (12b) is given by

$$\dot{V}_2 = -W_1(\eta) - k_2 \xi^2 + L_g V_1(\eta) \xi. \quad (29)$$

⁴It has been noticed, through intensive numerical simulations, that this pitfall cannot be avoided even by assigning different values for the design parameters k_1 and k_0 .

We now invoke the boundedness of $L_g V_1(\eta)$. Namely, it is readily shown that $L_g V_1(\eta)$ achieves its maximum at $z_2^* = \frac{2}{3}(P_S - x_{2N})$. That is,

$$M := \max_{\eta} L_g V_1(\eta) = \frac{2C_d W}{3\sqrt{3}\rho} (P_S - x_{2N})^{\frac{3}{2}}. \quad (30)$$

Combining (29) and (30) and exploiting the fact that (27) accomplishes the exponential convergence of ξ to zero,

$$\begin{aligned} \dot{V}_2 &\leq -W_1(\eta) - k_2 \xi^2 + M |\xi| \\ &= -W_1(\eta) - k_2 \xi^2 + M |\xi(0)| e^{-k_2 t}, \\ &\forall \{\eta, \xi\} \in \mathcal{D} \times [-x_{3N}, x_{3\max} - x_{3N}], \quad \forall t \geq 0. \end{aligned} \quad (31)$$

Based on (31), one concludes that \dot{V}_2 is negative definite outside a compact set, which in turn guarantees *uniform boundedness* of the solutions of (12). Furthermore, since the ‘disturbance’ in (31) converges to zero in addition to being bounded, control law (28) achieves convergence of all state variables to their equilibrium values as $t \rightarrow \infty$ (see §2.5.1 in [7] for the proof). A particular choice of design parameter $k_2 = 1/T$, reveals that the solutions of unforced system (11) are uniformly bounded and that they asymptotically converge to zero. Hence, when all parameters in (3) assume their nominal values, regulation control objective is achieved with $u = u_N$! This is a somewhat surprising discovery considering the overall complexity of the mathematical model of our system.

Figure 5 illustrates simulation results obtained using controller (28) with $k_2 = 50 \text{ s}^{-1}$, for the same values of x_{1N} and $x(0)$ as were used for controllers (25) and (26). Desired control objective is accomplished with very fast convergence of the control signal to its nominal value. Also much better output transient responses are obtained comparing to the results shown in Figure 3 and Figure 4. However, one cannot neglect the fact that simulation results were obtained for the case when all parameters are exactly known. Since controllers (25) and (26) provide a higher ‘degree of stability’ than their counterpart (28), they can be expected to work better in the presence of parametric uncertainties and/or unmodeled dynamics.

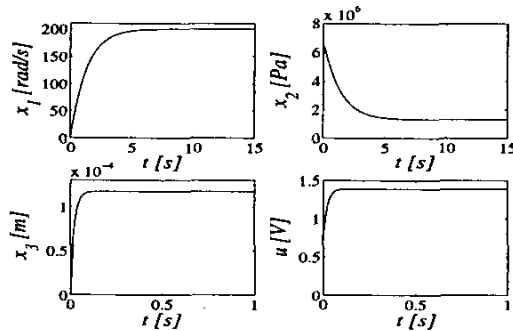


Figure 5: Simulation results of system (3) obtained using control law (28), for $k_2 = 50 \text{ s}^{-1}$, $x_{1N} = 200 \text{ rad/s}$, and $x(0) = 0$.

5 Concluding Remarks

This paper has dealt with the nonlinear control of a velocity EHSS consisting of an electrohydraulic servo-valve and an axial-piston hydraulic motor. The questions of relative degree and zero dynamics have been addressed and it has been shown that the system has a well defined relative degree, $r = 3$, and that it is minimum phase. These facts allow the design of a stabilizing control law based on feedback linearization. Due to the potentially harmful influence of cancellations in the presence of unmodeled dynamics and/or parametric uncertainties, several controllers have also been designed using the backstepping design procedure. By careful analysis of the dynamical properties of the system, the problem of unnecessary cancellations has been circumvented and controllers that guarantee a higher ‘degree of stability’ have been obtained. The Lyapunov function has been found to have a very simple quadratic form despite the complexity of the mathematical representation of the EHSS. Additionally, invaluable new insights have been gained about the dynamics of the system under consideration. This illustrates that the true potential of constructive nonlinear design lies far beyond the mere task of achieving a desired control objective.

Our current efforts are directed towards development of controllers that would provide desired robustness properties in the presence of inevitable modeling uncertainties.

Acknowledgments

The author is deeply indebted to Professor Petar Kokotović and Professor Andrew Teel for inspiring discussions and useful suggestions, and to Professor Bassam Bamieh for his support.

References

- [1] H. E. Merritt, *Hydraulic Control Systems*. New York: John Wiley & Sons, Inc., 1967.
- [2] J. Watton, *Fluid Power Systems*. New York: Prentice Hall, 1989.
- [3] B. Yao, F. Bu, J. Reedy, and G. T. C. Chiu, “Adaptive Robust Motion Control of Single-Rod Hydraulic Actuators: Theory and Experiments,” *IEEE/ASME Transactions on Mechatronics*, vol. 5, no. 1, pp. 79–91, March 2000.
- [4] A. G. Alleyne and R. Liu, “Systematic Control of a Class of Nonlinear Systems with Application to Electrohydraulic Cylinder Pressure Control,” *IEEE Transactions on Control Systems Technology*, vol. 8, no. 4, pp. 623–634, July 2000.
- [5] A. Isidori, *Nonlinear Control Systems*. Berlin: Springer-Verlag, 1989.
- [6] H. K. Khalil, *Nonlinear Systems*. New York: Prentice Hall, 1996.
- [7] M. Krstić, I. Kanellakopoulos, and P. Kokotović, *Nonlinear and Adaptive Control Design*. New York: John Wiley & Sons, Inc., 1995.
- [8] M. R. Jovanović, “Practical Tracking Automatic Control of Axial Piston Hydraulic Motors,” Master’s thesis, University of Belgrade, 1998.